Supporting Information for

"Mechanochemical Syntheses and ^{35}Cl Solid-State NMR Characterization of Fluoxetine HCl Cocrystals"

Austin A. Peach, David A. Hirsh, Sean T. Holmes, and Robert W. Schurko**University of Windsor, Department of Chemistry and Biochemistry, Windsor, Ontario, Canada N9B 3P4*

*Author to whom correspondence should be addressed. E-mail: rschurko@uwindsor.ca; Web: http://www.uwindsor.ca/schurko; Tel: (519) 253-3000 x3548; Fax: (519) 973-7098

Table of Contents:

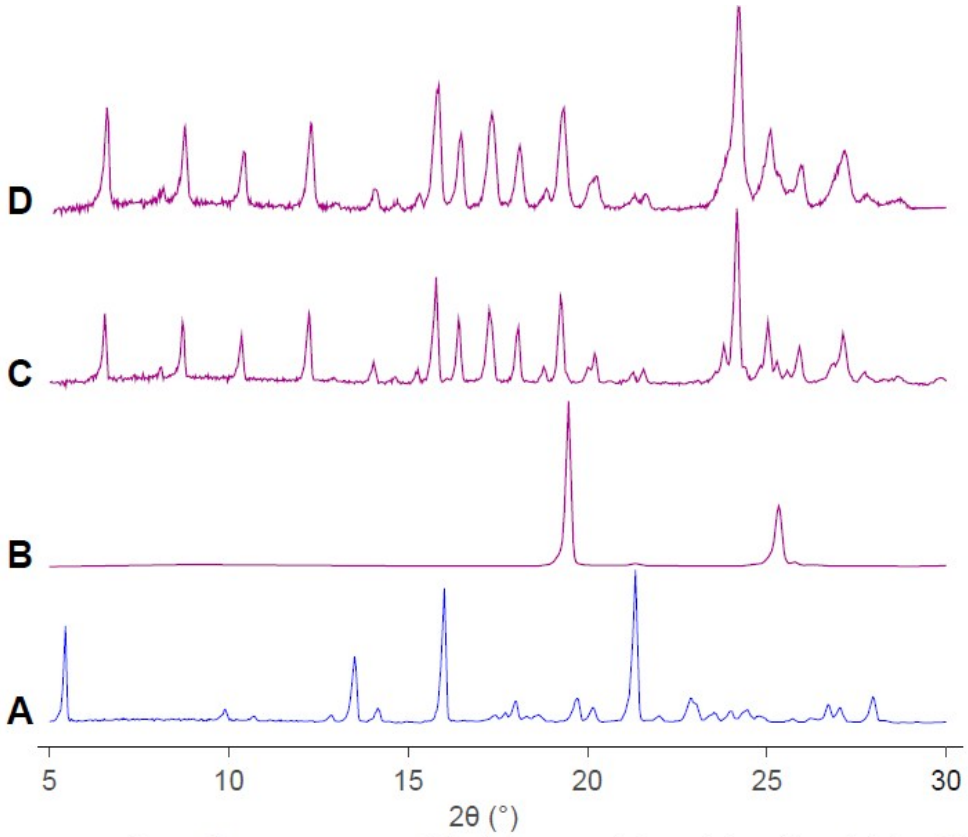

Figure S1. Experimental PXRD patterns of the (**A**) **Fluox**, (**B**) succinic acid, and (**C**) and (**D**) **Fluox$_2$Succ** cocrystal made using the **LAG** technique after a milling time of 30 minutes and of 5 minutes respectively (see text for more details).

Table S1. Static ^{35}Cl SSNMR acquisition parameters for the WURST-CPMG experiments at 9.4 T under static sample conditions.

	Fluox	$Fluox_2Fum$			FluoxBenz			$Fluox_2Succ$		
		SE	LAG	NG	SE	LAG	NG	SE	LAG	NG
Number of scans	28800	21600	21600	21600	21600	21600	21600	21600	21600	21600
Experimental time (h)	8	6	6	6	6	6	6	6	6	6
Recycle delay (s)	1	1	1	1	1	1	1	1	1	1
Number of echoes	75	80	80	80	150	150	150	100	100	100
Echo length (ms)	0.15	0.2	0.2	0.2	0.2	0.2	0.2	0.2	0.2	0.2
Dwell (μs)	0.5	0.625	0.625	0.625	0.5	0.5	0.5	0.667	0.667	0.667
Spectral width (kHz)	1000	800	800	800	1000	1000	1000	750	750	750
Acquisition length (number of points)	39630	40240	40240	40240	93980	93980	93980	47080	47080	47080
WURST pulse width (μs)	50	50	50	50	50	50	50	50	50	50
^{35}Cl WURST pulse rf (kHz)	15.6	15.6	15.6	15.6	15.8	15.8	15.8	15.8	15.8	15.8
Sweep range of WURST pulse (kHz)	500	500	500	500	500	500	500	500	500	500

Table S2. Static ^{35}Cl SSNMR acquisition parameters for the quadrupolar echo experiments at 21.1 T.

	Fluox	$Fluox_2Fum$			FluoxBenz			$Fluox_2Succ$		
		SE	LAG	NG	SE	LAG	NG	SE	LAG	NG
Number of scans	24576	24576	6144	–	24576	–	12288	–	6144	–
Experimental time (h)	14	14	3.5	–	14	–	7	–	3.5	–
Recycle delay (s)	2	2	2	–	2	–	2	–	2	–
Dwell (μs)	2	2	2	–	2	–	2	–	2	–
Spectral width (kHz)	250	250	250	–	250	–	250	–	250	–
Acquisition length (number of points)	1024	1024	1024	–	1024	–	1024	–	1024	–
90° pulse width [π/2] (μs)	3	3	3	–	3	–	3	–	3	–
^{1}H decoupling field (kHz)	30	30	30	–	30	–	30	–	30	–

Table S3. ^{35}Cl SSNMR acquisition parameters for the quadrupolar echo MAS experiments conducted at 21.1 T.

	Fluox	$Fluox_2Fum$			FluoxBenz			$Fluox_2Succ$		
		SE	LAG	NG	SE	LAG	NG	SE	LAG	NG
Number of scans	73728	57344	24576	–	–	–	59392	–	24576	–
Experimental time (h)	42	16	7	–	–	–	17	–	7	–
Recycle delay (s)	2	1	1	–	–	–	1	–	1	–
Dwell (μs)	2	2	2	–	–	–	2	–	2	–
Spectral width (kHz)	250	250	250	–	–	–	250	–	250	–
Acquisition length (number of points)	4096	4096	4096	–	–	–	4096	–	4096	–
90° pulse width [π/2] (μs)	3	3	3	–	–	–	3	–	3	–
Spinning speed (kHz)	31.25	31.25	31.25	–	–	–	31.25	–	31.25	–

Table S4. ^{1}H-^{13}C VACP/MAS SSNMR acquisition parameters for experiments conducted at 9.4 T on starting reagents.

	Fluox	Fumaric Acid	Benzoic Acid	Succinic Acid
Number of scans	3376	36	328	216
Experimental time (h)	9.4	1.2	7.3	4.8
Recycle delay (s)	10	120	80	80
Contact time (ms)	0.5	0.5	0.5	0.5
^{1}H Hartmann-Hahn matching field (kHz)	38.4	38.4	43.7	38.4
^{1}H $\pi/2$ pulse width (μs)	2.5	2.5	2.5	2.5
Dwell (μs)	8.4	8.4	8.4	8.4
Spectral width (kHz)	59.52	59.52	59.52	59.52
Acquisition length (number of points)	5120	5120	5120	5120
^{1}H decoupling field (kHz)	60	60	60	60
Spinning speed (kHz)	12	12	12	12

Table S5. ^{1}H-^{13}C VACP/MAS SSNMR acquisition parameters for experiments conducted at 9.4 T on HCl API cocrystals.

	$Fluox_2Fum$			FluoxBenz			$Fluox_2Succ$		
	SE	LAG	NG	SE	LAG	NG	SE	LAG	NG
Number of scans	280	652	432	208	1296	768	536	600	–
Experimental time (h)	4.7	10.9	7.2	1.7	10.8	6.4			–
Recycle delay (s)	60	60	60	30	30	30	30	30	–
Contact time (ms)	10	6	0.5	0.5	0.5	0.5	10	0.5	–
^{1}H Hartmann-Hahn matching field (kHz)	38.4	38.4	38.4	38.4	38.4	38.4	38.4	38.4	–
^{1}H $\pi/2$ pulse width (μs)	2.7	2.5	2.5	2.5	2.5	2.5	2.7	2.5	–
Dwell (μs)	8.4	8.4	8.4	8.4	8.4	8.4	8.4	8.4	–
Spectral width (kHz)	59.52	59.52	59.52	59.52	59.52	59.52	59.52	59.52	–
Acquisition length (number of points)	5120	5120	5120	5120	5120	5120	5120	5120	–
^{1}H decoupling field (kHz)	60	60	60	60	60	60	60	60	–
Spinning speed (kHz)	12	12	12	12	12	12	12	12	–

Table S6. ^{19}F MAS SSNMR acquisition parameters for the experiments conducted at 9.4 T on HCl API cocrystals.

	Fluox	$Fluox_2Fum$			FluoxBenz			$Fluox_2Succ$		
		SE	LAG	NG	SE	LAG	NG	SE	LAG	NG
Number of scans	256	-	256	-	-	256	-	-	256	-
Experimental time (h)	0.35	-	0.35	-	-	0.35	-	-	0.35	-
Recycle delay (s)	5	-	5	-	-	5	-	-	5	-
Dwell (μs)	3.33	-	3.33	-	-	3.33	-	-	3.33	-
Spectral width (kHz)	150	-	150	-	-	150	-	-	150	-
Acquisition length (number of points)	2048	-	2048	-	-	2048	-	-	2048	-
^{19}F π/2 pulse width (μs)	2.5	-	2.5	-	-	2.5	-	-	2.5	-
^{19}F Hahn-echo rf (kHz)	98.8	-	98.8	-	-	98.8	-	-	98.8	-
Spinning speed (kHz)	15	-	15	-	-	15	-	-	15	-

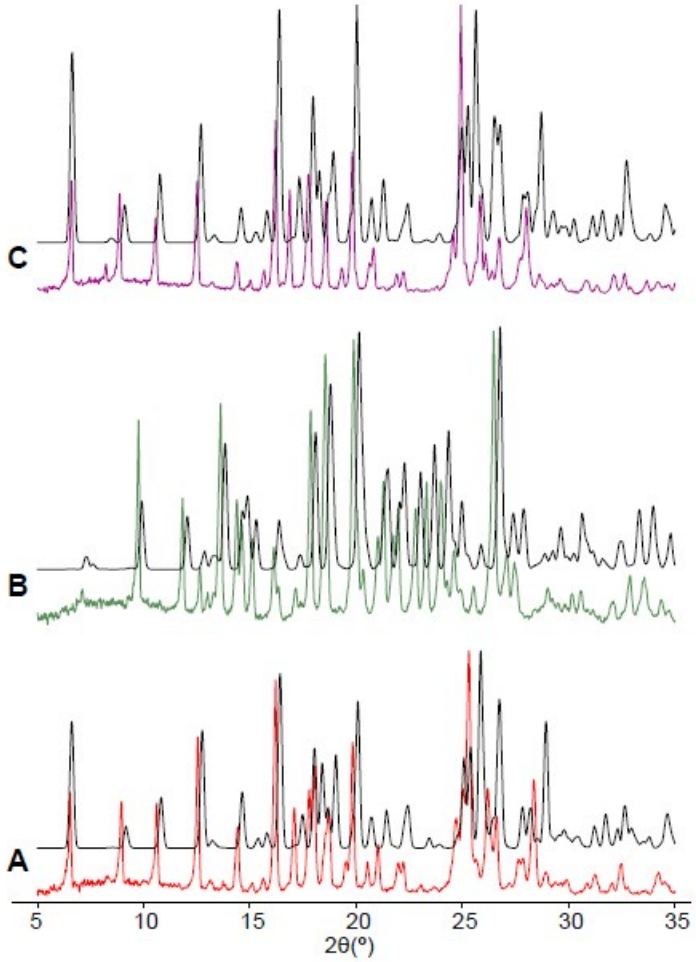

Figure S2. Experimental PXRD patterns of the three fluoxetine HCl cocrystals made using the **LAG** technique (**A**) **Fluox$_2$Fum**, (**B**) **FluoxBenz**, and (**C**) **Fluox$_2$Succ** (lower traces), and corresponding analytical simulations (upper traces). Analytical simulations are based on single crystal structures obtained at 100 K, whereas experimental patterns were obtained at 293 K. Descrepencies between experimental and analytical simulations are due to unit cell contractions.

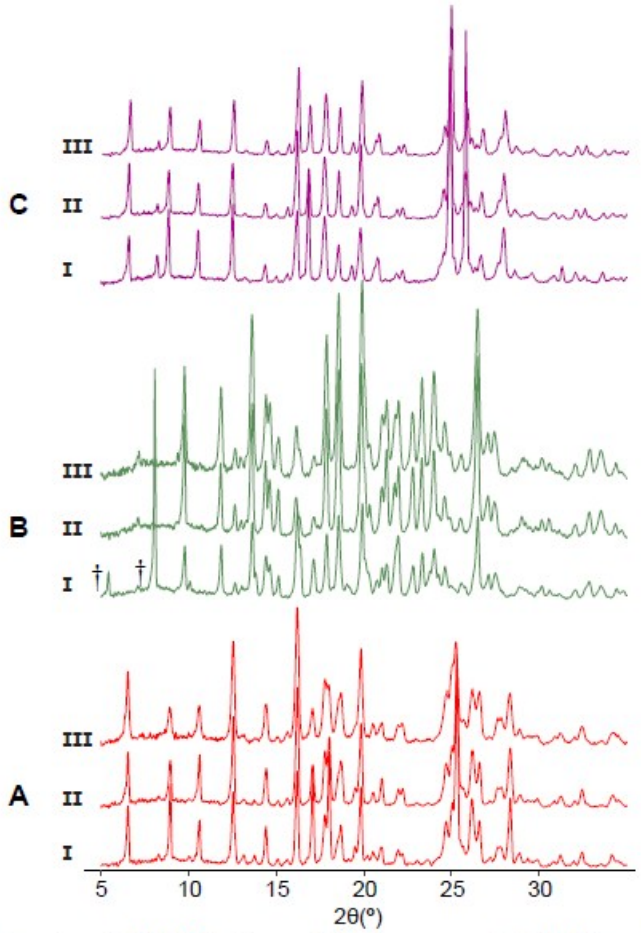

Figure S3. Experimental PXRD patterns of the three cocrystals (**A**) **Fluox$_2$Fum**, (**B**) **FluoxBenz**, and (**C**) **Fluox$_2$Succ**, as prepared by (**I**) slow evaporation (**SE**), (**II**) liquid assisted-grinding (**LAG**), and (**III**) neat grinding (**NG**). Impurity peaks are marked with † (see text for details).

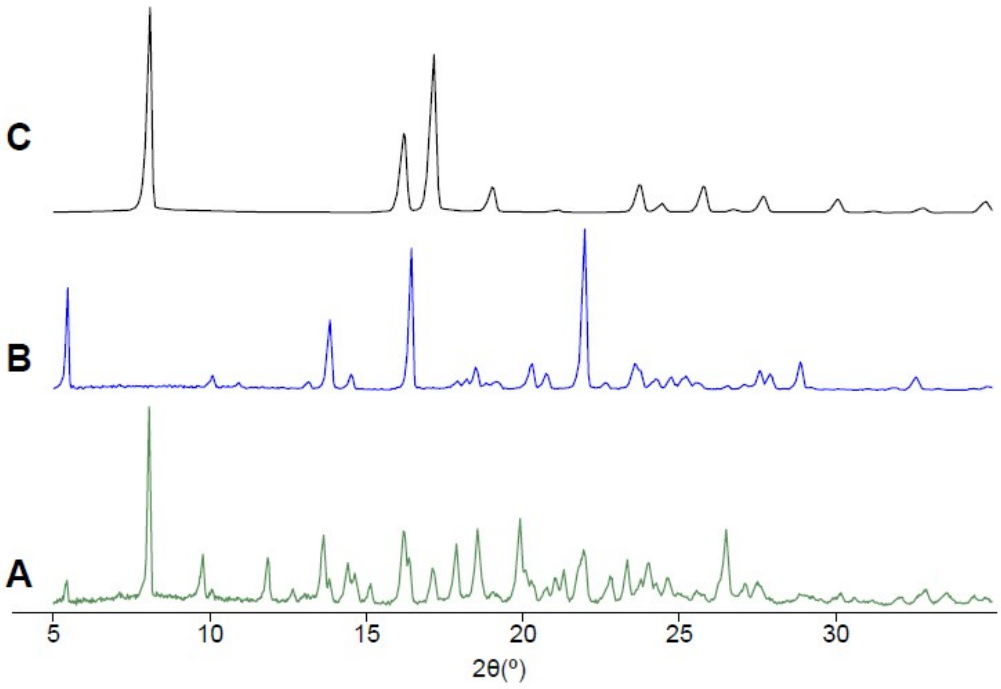

Figure S4. Experimental PXRD patterns of (**A**) **FluoxBenz**, (**B**) **Fluox**, and (**C**) benzoic acid.

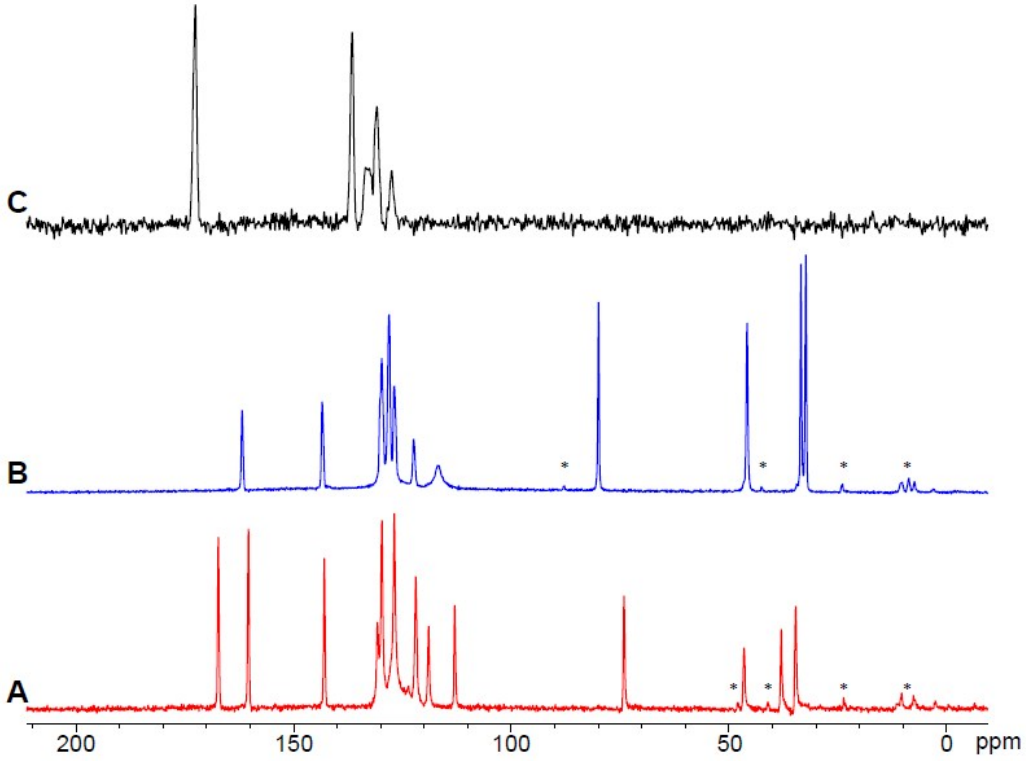

Figure S5. ^{1}H-^{13}C CP/MAS (ν_{rot} = 12 kHz) SSNMR spectra acquired at B_0 = 9.4 T of (**A**) **Fluox$_2$Fum** (synthesized by **LAG**), (**B**) **Fluox**, and (**C**) fumaric acid. Spinning sidebands are indicated with asterisks (*).

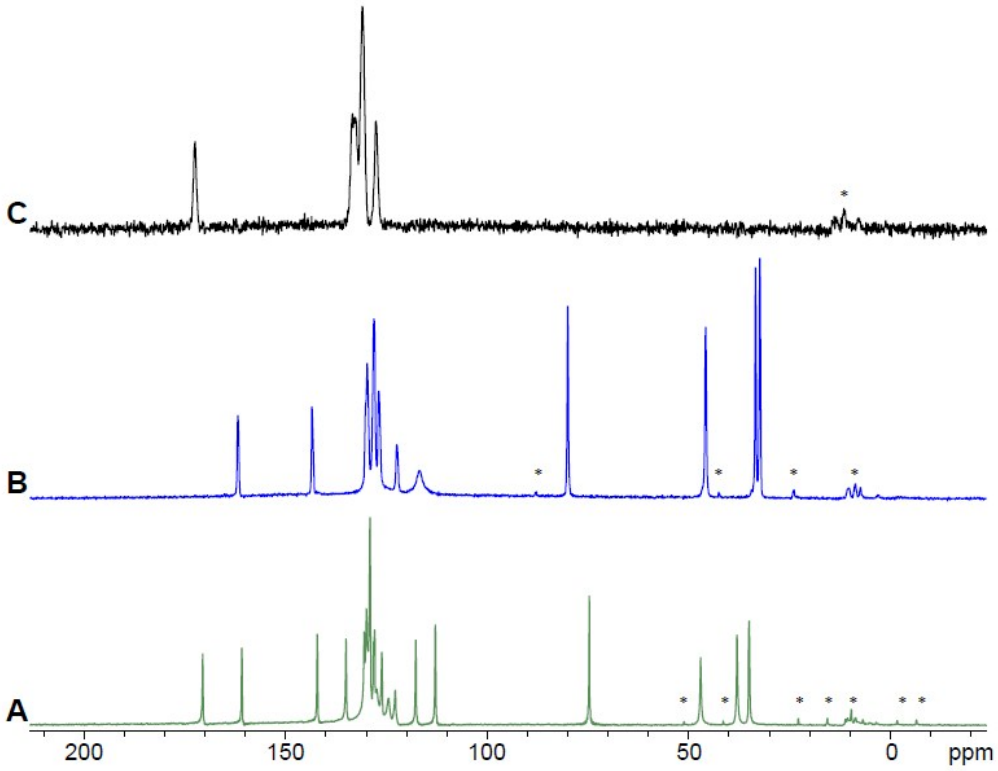

Figure S6. ^{1}H-^{13}C CP/MAS (ν_{rot} = 12 kHz) SSNMR spectra acquired at B_0 = 9.4 T of (**A**) **FluoxBenz** (synthesized by **LAG**), (**B**) **Fluox**, and (**C**) benzoic acid. Spinning sidebands are indicated by asterisks (*).

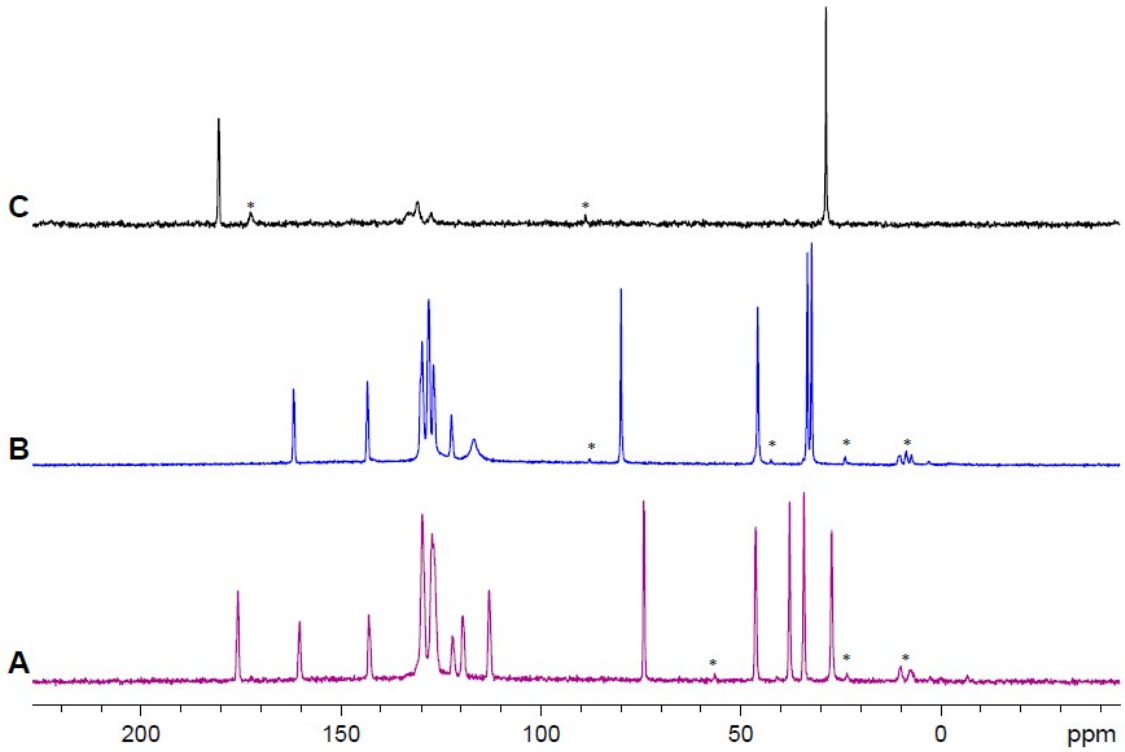

Figure S7. ^{1}H-^{13}C CP/MAS (ν_{rot} = 12 kHz) SSNMR spectra acquired at B_0 = 9.4 T of (**A**) **Fluox$_2$Succ** (synthesized by **LAG**), (**B**) **Fluox**, and (**C**) succinic acid. Spinning sidebands are indicated with asterisks (*).

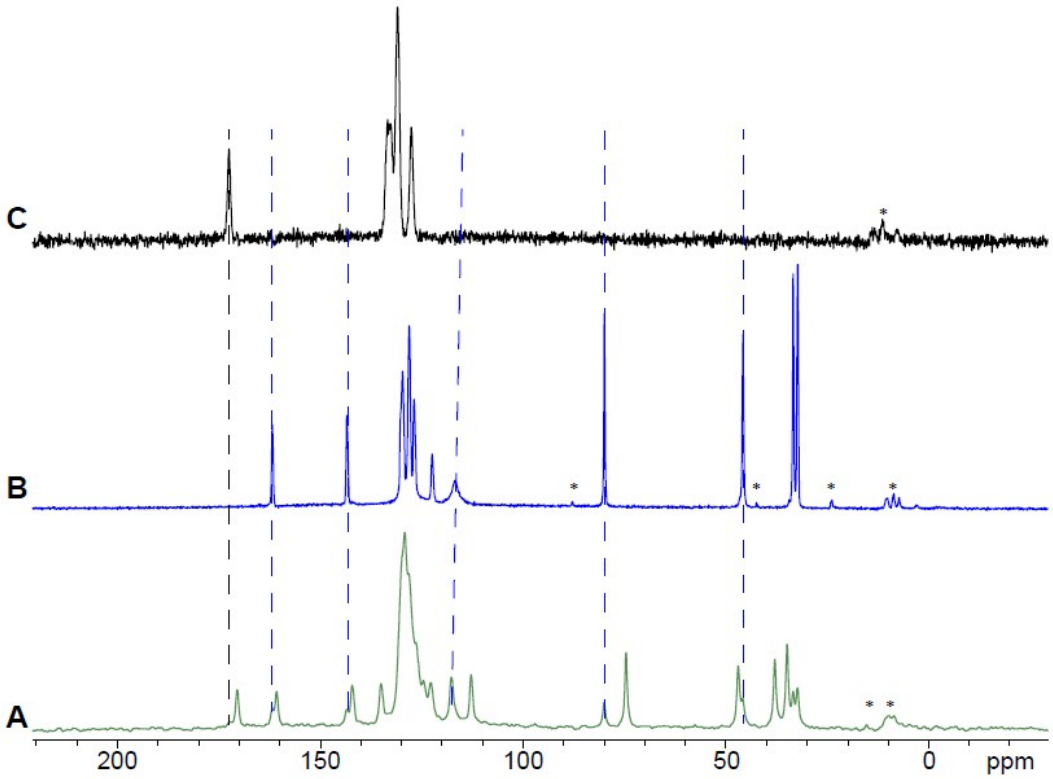

Figure S8. ^{1}H-^{13}C CP/MAS (ν_{rot} = 12 kHz) SSNMR spectra acquired at B_0 = 9.4 T of (**A**) **FluoxBenz** (synthesized by **SE**), (**B**) **Fluox**, and (**C**) benzoic acid. Spinning sidebands are indicated by asterisks (*). Dashed lines in blue and black denote starting material impurites from spectra of **B** and **C**.

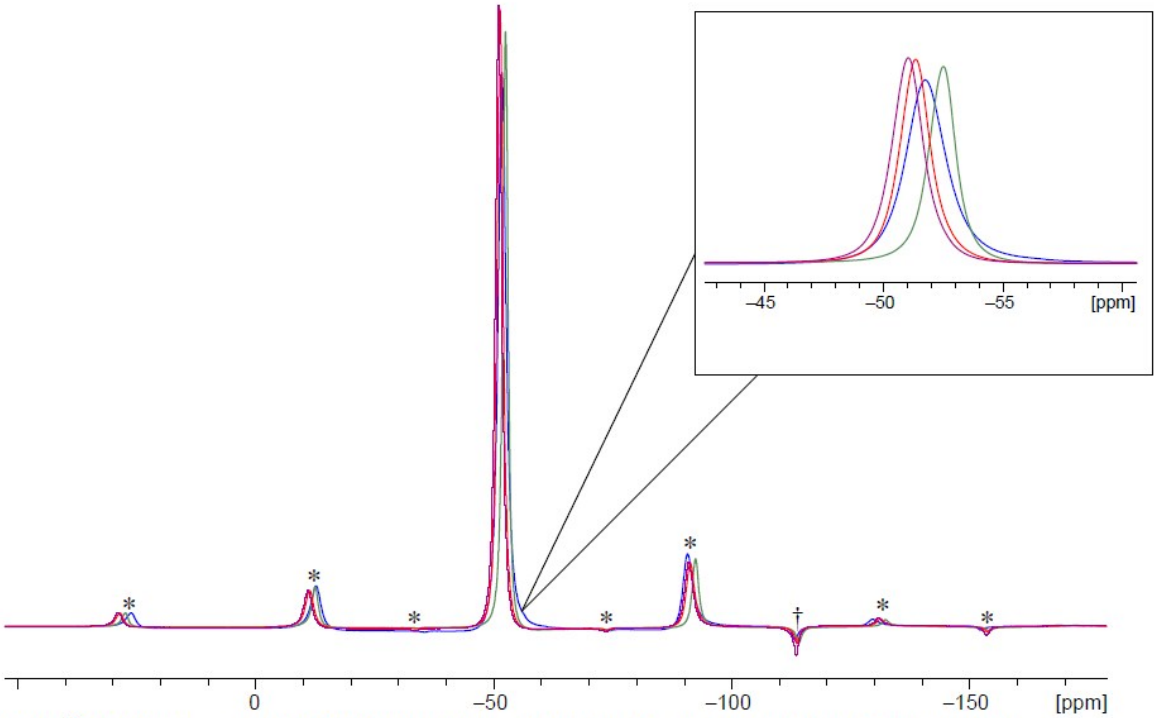

Figure S9. ^{19}F MAS (ν_{rot} = 15 kHz) SSNMR spectra acquired at B_0 = 9.4 T. Shown in the inset are the isotropic peaks of the cocrystals synthesized by **LAG** of **Fluox$_2$Succ** (purple), **Fluox$_2$Fum** (red), **Fluox** (blue), and **FluoxBenz** (green). Spinning sidebands are indicated with asterisks (*). Background signal from teflon is denoted by (†). N.B the crystal structure of FluoxBenz suggests 2 asymmetric fluoxetine molecules and only one isotropic shift, not two, is observed.

A simple point charge analysis was used to rationalize the orientations of the principal values of the ^{35}Cl EFG tensors associated with the chloride anions of fluoxetine HCl and 2:1 fluoxetine HCl:benzoic acid. A more detailed discussion of this type of analysis is provided by Knop (*Acta Crystallogr.*, **1975**, *31*, 19-31). Such a model simplifies the full quantum mechanical description of the solids to a series of atom-centered point charges; consequently, this approach is used only to supplement and aid in the interpretation of the dispersion-corrected DFT results.

In the present analysis, the Cartesian coordinates of the point charges are labeled x_i, y_i, and z_i, the distances from the chloride anion is labeled r_i, the magnitudes of the charges are labeled u_i, and the elements of the 3 x 3 matrix are given by the summation over U_{xx}, U_{xy}, etc. Here, $U_{i,xx} = u_i r_i^{-5}\left(3x_i^2 - r_i^2\right)$, $U_{i,xy} = 3u_i r_i^{-5} x_i y_i$, and $r_i = \left(x_i^2 + y_i^2 + z_i^2\right)^{1/2}$. The positions of all atoms were obtained from the DFT-D2* refined structures and the atomic charges were chosen since these are typical values in Mulliken population analyses. An example analysis for fluoxetine HCl (Table S7) illustrates the values from which the EFG tensor can be constructed, and subsequently diagonalized to obtain the eigenvalues and eigenvectors. A model in which the ^{35}Cl EFG tensor originates from the point charges associated with the nine nearest atoms predicts an orientation of V_{33} which is consistent with the DFT-D2* calculations. In contrast to this result, when considering only the N atoms and the two H atoms participating in hydrogen bonding (H10 and H11), V_{33} points near both of the hydrogen-bonding axes (N.B. the H-Cl-H angle is greater than 170°). From this, it is evident that the orientations of the principal values of the ^{35}Cl EFG tensor in fluoxetine HCl are highly sensitive to weak intermolecular interactions. Similar analyses can be used to predict the orientation of V_{33} in the cocrystals using the atomic coordinates from the attached .cif files.

Table S7. Point charge analysis of the ^{35}Cl EFG tensor in fluoxetine HCl.

Atom label	u_i	x_i	y_i	z_i	r_i	$U_{i,xx}$	$U_{i,yy}$	$U_{i,zz}$	$U_{i,xy}$	$U_{i,xz}$	$U_{i,yz}$
H2	0.25	-1.598	2.037	1.211	2.859	-0.001	0.006	-0.005	-0.013	-0.008	0.010
H4	0.25	1.238	-1.697	-1.755	2.738	-0.005	0.002	0.003	-0.010	-0.011	0.015
H9	0.25	-0.491	-1.093	2.660	2.917	-0.009	-0.006	0.015	0.002	-0.005	-0.010
H10	0.25	-1.754	-1.170	-0.398	2.145	0.025	-0.003	-0.023	0.034	0.012	0.008
H11	0.25	1.911	0.988	0.127	2.155	0.034	-0.009	-0.025	0.030	0.004	0.002
H13	0.25	-1.841	1.972	-1.159	2.936	0.002	0.003	-0.005	-0.012	0.007	-0.008
H14	0.25	1.722	-2.146	0.441	2.787	0.002	0.009	-0.011	-0.016	0.003	-0.004
N1	-0.5	-2.524	-1.751	-0.568	3.123	-0.016	0.001	0.015	-0.022	-0.007	-0.005
N1	-0.5	2.705	1.557	0.074	3.122	-0.021	0.004	0.016	-0.021	-0.001	-0.001